Final Report

CS 224W
Prof. Leskovec
Teammates: Scotty Fleming, Cooper Raterink, Zach Taylor
Submit Date: 12/09/18

1 Abstract

In recent years, advances in functional magnetic resonance imaging (fMRI) have given us a unique insight into patterns of activity in the human brain. Traditionally, fMRI data have been used to make claims about the general architecture and strength of connections between different regions of the human brain. More recently, heterogeneity in individuals' connectomes have been implicated in neurological and psychiatric disorders, like Depression and Anxiety. Careful data-driven parcellations of the brain have given rise to discrete brain regions of interest, which can be conceptualized as nodes in a network. Functional connectivity between these nodes can be derived from the fMRI time-series, representing edges and edge weights in a brain connectome network. However, this network is plagued by biological noise. In this project, we propose a framework of denoising and subsequent topological analysis that aims to be relatively robust to such data artifacts. This framework is then applied in a real world dataset to explore, under several different network topological representations, (1) the degree to which patterns of variation in individuals' brain networks persist over time and can uniquely identify an individual and (2) whether these patterns of variation distinguish patients with emotional disorders from healthy controls. We also explore whether robustness measurements can be used to distinguish healthy and depressed brain networks.

2 Background and Motivation

2.1 Problem Background

The human brain represents an extraordinarily complex network, comprising one hundred billion neurons, each connected to an average of 7,000 other neurons through junctions called synapses. This yields between 100 trillion and 1 quadrillion synapses total in the human brain, depending on a person's age [4]. Current research in psychology and neuroscience suggests that it is the architecture and dynamic interactions of neurons in the brain that give rise to cognition [17]. Analyzing networks in the brain therefore offers a unique opportunity to better understand how complex behavioral phenomena like emotions arise [1].

While understanding the basic architecture and dynamics of the human brain network is an important scientific question in its own right, there are more immediately translational questions that can potentially be answered using modern network analysis techniques. Specifically, disruptions in functional network architectures in the brain have been associated with disorders like Major Depressive Disorder (MDD) in the literature [14]. These associations suggest rich and fruitful opportunities for research comparing network characteristics of patients with MDD to healthy controls. The variety of documented network analysis techniques actually employed in characterizing such differences, however, is surprisingly narrow.

Research in the last decade has used network characteristics like path length, [2], clustering coefficients, and community detection [10] to yield an insightful picture into the small-world, rich-club organization of the brain [18]. A few papers have explored topology in structural and functional brain networks of healthy individuals [16] and elucidated the role that certain toplogical characteristics might play in sustaining network activity and modulating network

synchronization, both of which are thought to be fundamental to a wide array of cognitive processes [6] [12] [8] [9]. Given its supposedly important role in cognition, one might imagine that disruptions in topology across the brain network could be implicated in mood disorders like MDD; however, we could not find any literature to date either supporting or refuting such an association.

2.2 Problem Scope

As there are potentially infinite types of metrics one could use to characterize an individual's functional connectome network, one must be judicious in selecting and testing candidate metrics; given the large space of possible network representations and associated metrics, one could easily find a measure that demonstrates a spuriously "significant" difference between patients with emotional disorders and healthy controls. This is especially true under our context of a finite and relatively small sample size. To that extent, we make the assumption that, if there does exist a network measure that distinguishes patients with emotional disorders from healthy controls, then it is likely to be one that does not change substantially within an individual over the course of hours, days, or even weeks. More specifically, if we have such a reliable measure $f(G_i)$ that takes in a functional connectome of subject i, namely G_i, and returns a lower-dimensional vector representation, we would expect that the position of $f(G_i)$ relative to $f(G_j)$ for all $j \neq i$ would be fairly constant after hours, days, or weeks. Indeed one might imagine that, given scans from the same set of individuals at two time points, t_0 and t_1 one would be able to uniquely identify who is who at time t_1 based on the representation at time t_0.

A recent paper by Finn et al. (2015) demonstrated a promising first step in this direction, showing that using an individual's densely connected functional connectome and its associated edge weights, they could uniquely distinguish individuals one from another in a second scan based on the results of the first with accuracy close to 100% [5]. These findings suggest that finding a persistent, trait-like (rather than ephemeral or state-like) representation of the functional connectome is not unreasonable. What remains to be seen is whether lower-dimensional topological representations could also uniquely and reliably identify individuals in a retest scenario and whether such a representation relates in any meaningful way to the presence or absence of emotional disorders.

In this project, we explore (1) the natural variance in the topological structure of functional connectomes among healthy individuals and how stable differences are over time, as well as (2) the degree to which disruptions in the frequency of certain graphlets and associated topology in the brain's functional connectome differs between healthy individuals and individuals with Major Depressive Disorder (MDD). We use data on 23 subjects from the original Human Connectome Project to find a topological network representation that can uniquely identify individuals and is persistent/reliable over time, and we use data on a separate set of 100 subjects from the associated Mapping Connectomes for Disordered Mental States project at Stanford to test whether there are significant differences between MDD patients and healthy controls under this representation. Approximately one-sixth of subjects in the Stanford cohort are healthy individuals, while the rest suffer from one or more symptoms of "acute threat, loss of reward valuation/responsiveness, and/or difficulties in working memory" [11]. For each individual in the dataset we construct their functional connectome using resting state fMRI (rsfMRI) data. Resting state fMRI data consist of multiple snapshots of a persons brain activity while they are presented with a neutral stimulus (i.e. staring at a white dot on a black screen).

Nodes are defined using regions given in the Glasser parcellation (consisting of 360 regions in the brain, as described later in the preprocessing section). Following Finn et al. (2015), we begin with the assumption of a densely connected network and define edge strengths as the correlation between the activation patterns in pairs of nodes over time [5]. In order to obtain sparsity in the graph representation, we use a hard thresholding/sparsification technique described later in the preprocessing and methods sections. The remaining edges are binarized [13], resulting in a relatively sparse, unweighted and undirected network representing each individual's connectome. This work serves to answer an important question about whether topological properties of the human functional connectome, as measured by graphlet degree distribution, are associated with mood disorders like depression.

3 Data Collection Process

We used data from the Human Connectome Project (HCP) for our analyses. The HCP is public, and consists of 1113 subjects with fMRI data. We chose to use a subset of this population that had both test and retest data (so that we could evaluate whether the network representations we were testing were reliable/persistent over time, as described in the introduction). This narrowed down the population to 50. We then filtered out subjects with quality control issues as documented by the HCP, as well as any subjects with missing data. This gave us a sample of 23 subjects. We plan to utilize the full dataset as an extension, but started with this for storage reasons.

As a brief introduction, fMRI data is obtained using Magnetic Resonance Imaging and measures the Blood Oxygen Level Dependent (BOLD) response in the brain. This response correlates with neural activity in an established way, and allows for the determining of which regions are highly correlated with each other in terms of temporal neural activity on a second-by-second time scale. Each subject's fMRI data consists of three-dimensional scans taken repeatedly over many time points.

For each subject, the dataset contains fMRI scans from 4 separate sessions with a combined 1200 total time points per subject. The first two sessions are close together in time, and contain different orientations to avoid associated biasing effects. The next two sessions have a similar setup but at a later time point on the same day.

Seeing as each subject's fMRI consists of four dimensions (three dimensional space with an added temporal dimension) and multiple sessions, the scale of the data presents a challenge for collection. Each patient's data comprises approximately 5 gigabytes of memory. Our initial sample is very narrowed down compared to the full dataset, but since we plan on using the full data eventually (which is roughly 3.9 terabytes for the sample we're interested in), we decided to utilize server space to store the Connectome data. The scale of the data made the developers of HCP decide to require the use of the *Aspera* plugin for any and all downloads. The plugin is useful in that it maximizes utilization of bandwidth, but it presented a challenge to use, since it turned out to be extremely unreliable on our particular servers and was difficult to install on Linux and with Firefox, which was the only browser supported with Linux systems. We eventually succeeded in downloading the data to the server with *Aspera*.

4 Preprocessing

There are a number of preprocessing steps necessary to transform raw fMRI connectivity values stored in .nifti files into a form that is suitable for network analysis. First, we installed the Human Connectome Workbench software on the server, and with it, executed a Matlab script to de-trend, normalize, and concatenate fMRI session data for each patient in our sample. The de-trending is necessary to remove noise, such as linear drift, that is caused by factors unrelated to the patient's brain and can obscure the more interesting patterns in the data. We concatenated the fMRI session data in order to obtain a larger sample, as samples that include more time in the scanner are more robust.

The next step in the preprocessing pipeline was parcellation. The idea behind cortical parcellation is that mapping the brain into its major subdivisions, or cortical areas, provides the most biologically meaningful level of granularity at which to analyze the data. Voxels (volume elements which make up a brain volume image) have such a small scale that their values aren't always robust across time unless they are smoothed with neighbors or parcellated. However, we also want to capture differences between regions with as much granularity as possible. The Glasser parcellation [7] that we used does this by delineating regions that are optimized to be distinct in terms of function, cortical architecture, connectivity, and topography. The parcellation takes the coordinates of the brain and maps them to one of 360 distinct parcels, giving us a more meaningful representation of the connectivity data.

Next, we used a sparsification technique to reduce the number of edges in our graph. The motivation for this, and a more detailed discussion, are provided in the methods section since it is an important part of the graph-theoretic analysis.

Finally, for our graphlet analysis discussed later, we further preprocessed the connectivity matrices in order to obtain graphlet degree distributions for each subject. We used an implementation of an algorithm called "ORCA" (the Orbit Counting Algorithm, which can be found on Github here). This orbit-counting performs a graphlet degree distribution analysis of the networks - it follows procedures that can be found in a paper on complex networks published by Natasa Przulj [20].

The paper also provides code for comparing two networks based on the resulting graphlet distribution features in terms of various distance metrics, so we chose to maintain solidarity with their methods and also use their network comparison code (which can be found at this website). They provide multiple options for distances - we chose to examine the performance of each of these on our datasets. The results can be found in Table 1.

5 Methods

5.1 Robustness

For part of our network topological analysis of brain-connectivity matrices we chose to look at how robust these brain networks are to edge removal. To measure robustness, we examine how the size of the largest strongly connected component (SCC) grows with respect to adding 20,000 edges in order of decreasing weight to individuals' graphs. The reason we chose 20,000 edges is because for each participant this gave us a portion of the curve well into the asymptotic range.

The algorithm is as follows:

Algorithm 1 Collect SCC size data

procedure SccSizeVsRemovedEdges(n-by-n $connMat$, int $stride$, int $numStrides$)
  $edgesByWeight \leftarrow argSortReverse(connMat)$
  $G \leftarrow$ empty graph with n nodes
  $sizes \leftarrow [\,]$
  $edgeI \leftarrow 0$
  for $1 \rightarrow numStrides$ **do**
    append $MaxSCCSize(G)$ to $sizes$
    for $1 \rightarrow stride$ **do**
      add $edgesByWeight[edgeI]$ to G
      $edgeI \leftarrow edgeI + 1$
  Return $sizes$

5.2 Toplogical Graphlet Analysis

In all, we collected connectivity matrices for 23 participants at both a test date and a follow-up retest date, each with 2 sessions, for a total of 92 connectivity matrices. The connectivity matrices were each pulled into a 379-by-379 numpy array, where element (i, j) represents the time-correlation of parcel i and parcel j, which is conventionally used in research as a proxy for the degree to which the two areas of the brain associated with parcels i and j are connected.

With these ninety-two $379-by-379$, float-valued, non-zero numpy arrays, We sought to do a network-topological analysis to determine a way of predicting (1) which participant a session-2 connectivity matrix was collected from, given all of the session-1 matrices (where both sessions were within the original test day); and (2) which participant a session-1 connectivity matrix was collected from on the retest date, given all of the session-1 matrices from the test date. Thus, we needed to convert these matrices to undirected, unweighted adjacency matrices for topology analysis. We chose to use a simplistic threshholding algorithm for this step.

The thresholding algorithm takes a connectivity matrix C and finds an "edge selection matrix" S to maximize:

$$\sum_{(i,j)} S_{i,j} C_{i,j} \tag{1}$$

Subject to the constraint:

$$\frac{\sum_{(i,j)} S_{i,j}}{|E|} \leq p \tag{2}$$

where $S_{i,j} = 1$ if we keep the edge, and $S_{i,j} = 0$ otherwise. Here p is the "density" the network representation of the connectivity matrix, and is equivalent to the percentage of edges kept. The algorithm keeps the highest-weighted p percent of edges. The "sparsified" resulting matrix is then just the $S_{i,j}$. Note that, in the case where there are at least $p|E|$ edges, this maximization procedure guarantees that the number of edges will be the same across all networks, assuming they begin with the same number of nodes (as is the case for our analysis). This allows to confidently compute unnormalized metrics based on graphlet frequencies rather than just proportions, for example.

After threshholding, we chose to analyze the topology of the resulting networks using graphlet distributions of size 5 or less. We used the ORCA algorithm described in the preprocessing

section to obtain graphlet degree distributions, along with ORCA's functionality for computing distances using various distance metrics over the resulting vectors. Distance metrics we tried include the Graphlet Correlation Distance (GCD), the Relative Graphlet Frequency Distance (RGF), the arithmetic and geometric Graphlet Degree Distribution Agreement Distances (GDD-A and GDD-G) [20]; a spectral distance metric using the eigenvalues of the network's Laplacian graph matrix [3]; and several other distance metrics based on network properties like degree distribution, clustering coefficients, and network diameter. While space does not permit an exhaustive treatment of these metrics, a comparison of their relative performance on the task at hand is given in Table 1.

The result of the ORCA code coupled with the distance comparison code gave us a distance matrix D for each distance metric. The $(i, j)th$ element of D is the measure of the distance between participant i's session-1 sparsified connectivity matrix and participant j's session-2 sparsified connectivity matrix (or participant i's test day and participant j's retest day connectivity matrices, respectively). We then computed the classification accuracy $acc(D)$ with the following algorithm:

The classification accuracy algorithm takes in a $N \times N$ (here $N = 23$) distance matrix D and a parameter k and produces a top-k accuracy (namely, the proportion of times the correct result is in the top k predictions of our model). First, we compute a $N \times k$ "minimum-distance" matrix M such that the $(i, j)th$ element of M is the index of the jth-smallest value in row i of D. We then compute the classification accuracy of D:

$$acc(D) = \frac{\sum_{i=1}^{N} \mathbb{1}\{i \epsilon M_{i,:}\}}{N} \tag{3}$$

After finding the representation which yielded the best model for predicting an individual's identity in a future scan based on a previous scan - a proxy for how persistent, or trait-like, the representation is - we examined the degree to which depressed patients differed from healthy controls under this representation. Specifically, after finding that a 73-dimensional graphlet degree vector yielded the highest predictive accuracy (see Results section below), we ran a t-test on the graphlet frequencies for each of the 73 automorphic orbits [20] comprising the graphlet degree vector to determine whether any of these distributions differed significantly between depressed subjects and health controls. We used Bonferroni Correction at level $\alpha = 0.05$ to correct for multiple hypothesis tests. Thus tests with a p-value smaller than 0.05 after controlling the Family Wise Error Rate (FWER) were considered significant.

5.3 Network Enhancement

Network Enhancement is a recently developed method by [19] that has shown to be effective in denoising weighted biological networks. Since our project focuses on fMRI data, which is both noisy and biological, we chose to try Network Enhancement as part of preprocessing pipeline. We analyzed the performance of our motif analysis algorithm both with and without Network Enhancement. We hypothesized that the predictive performance of our model would improve with network enhancement.

6 Results and Discussion

6.1 Robustness

Figures 1 and 2 below together show that although network robustness seems to be an interesting measure in our dataset (that is, it could be related to some other aspect of the human mind besides depression - although this needs further analysis), it cannot be used to either identify individuals across different fMRI sessions nor detect depression.

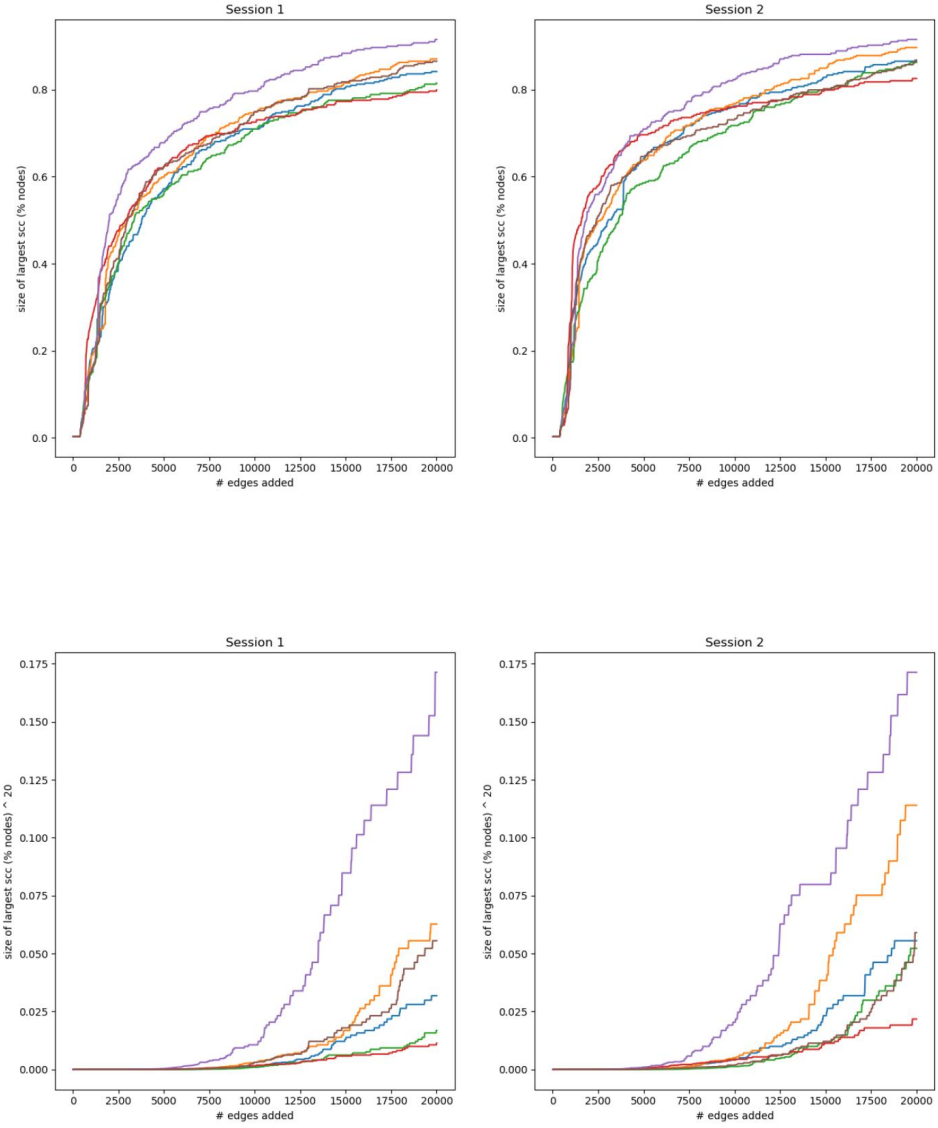

Figure 1: These graphs show the change in size of the SCC with respect to number of edges added to the graph (they are added by order of decreasing weight, beginning with the edge of highest weight). The top graphs show a normal y scale, and the bottom graphs show the percentage raised to the 20th power for visualization purposes. The same color corresponds to the same participant. You can see that there seems to be some correlation between the curves across sessions, but there is not enough to distinguish between participants.

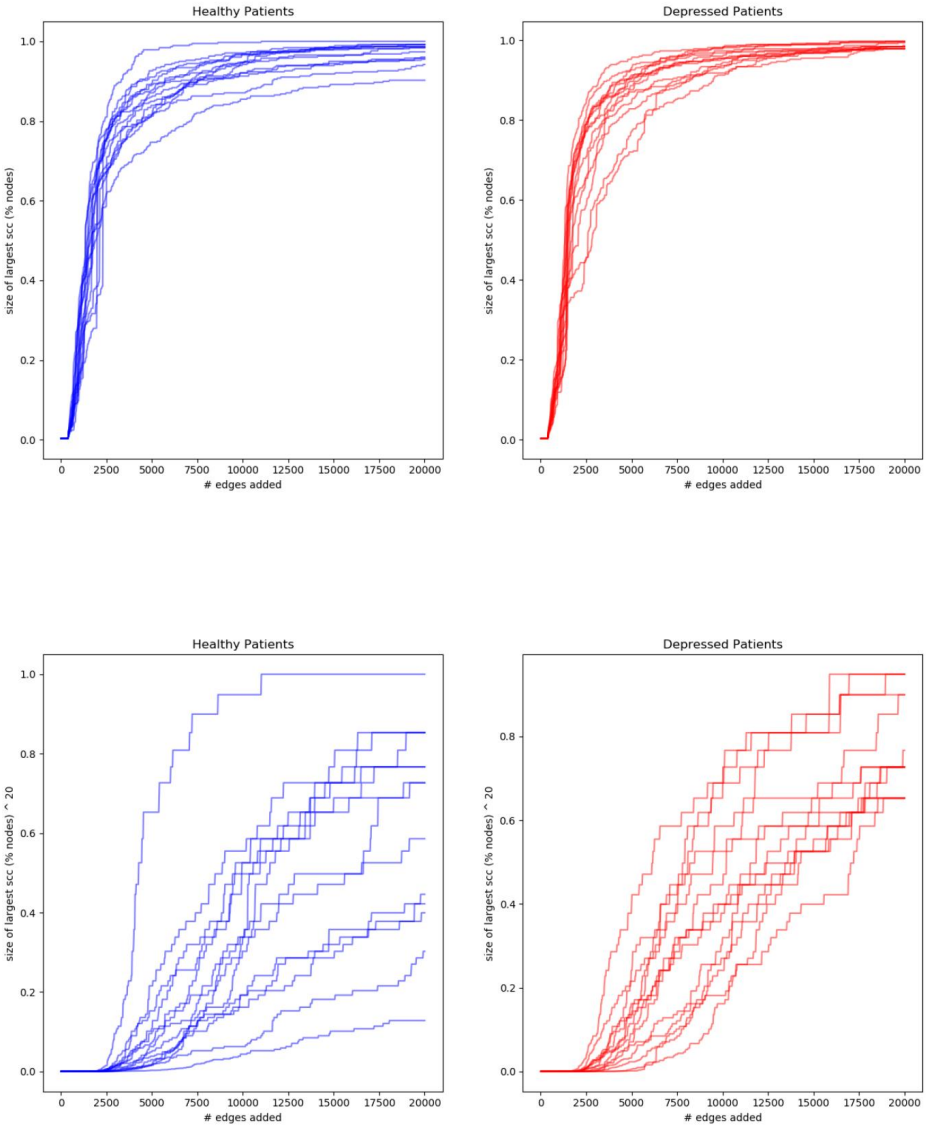

Figure 2: See Figure 1 for graph and scaling explanation. You can see that there seems to be a difference in the robustness profiles of healthy and depressed populations, but no obvious way to predict depression given just a robustness curve. It surprised us to see the robustness of healthy individuals had higher "variance" than that of the depressed. Perhaps the robustness curve measures some other aspect of the human mind.

6.2 Graphlet Analysis

Table 1 summarizes the results from our graphlet analysis, measuring the top-k accuracy for various values of k, utilizing several types of distance metrics, with and without network enhancement, and for the two types of tasks previously discussed (predicting session-2 scan identities from session-1 scan identities and retest scan identities from test scan identities). Graphlet degree vector representations and their associated distance metrics consistently outperformed other representations/distance metrics. Specifically, in examining the top-1 accuracy for our predictive analysis, we find that the Relative Graphlet Frequency distance (RGF) achieved

the highest accuracy at 0.24 in predicting session 2 from session 1 within a single test day, while Graphlet Correlation Distance using all 2-to-5 node graphlet orbits (GCD-73) yielded perfect top-1 accuracy in identifying individuals' retest scans from their test scans. Notably, even a small, 11-dimensional representation and graphlet-based distance metric (GCD-11) was sufficient to uniquely identify individuals' retest identities from their test scans.

Interestingly, network enhancement did not improve predictive performance at all except in one instance (predicting session 2 from session session 1 using a distance metric based on network diameter) in which case the gains from network enhancement were only marginal. This was surprising, giving its powerful demonstrations in the associated expository paper [19]. These discrepancies may be due, however, to the fact that changes under network enhancement make the underlying structure stand out more clearly from the noise, but do not necessarily alter the fundamental network topology. To the extent that the graphlet degree distribution can effectively extract signal from noisy networks to capture the underlying topology, we might expect the ameliorative effects of network enhancement to be more limited.

Altogether, these findings highlight a promising and exciting insight: they suggest that graphlet degree distributions truly do capture a trait-like characteristic of the functional connectome, sufficiently to uniquely characterize and identify an individual even after significant time has passed.

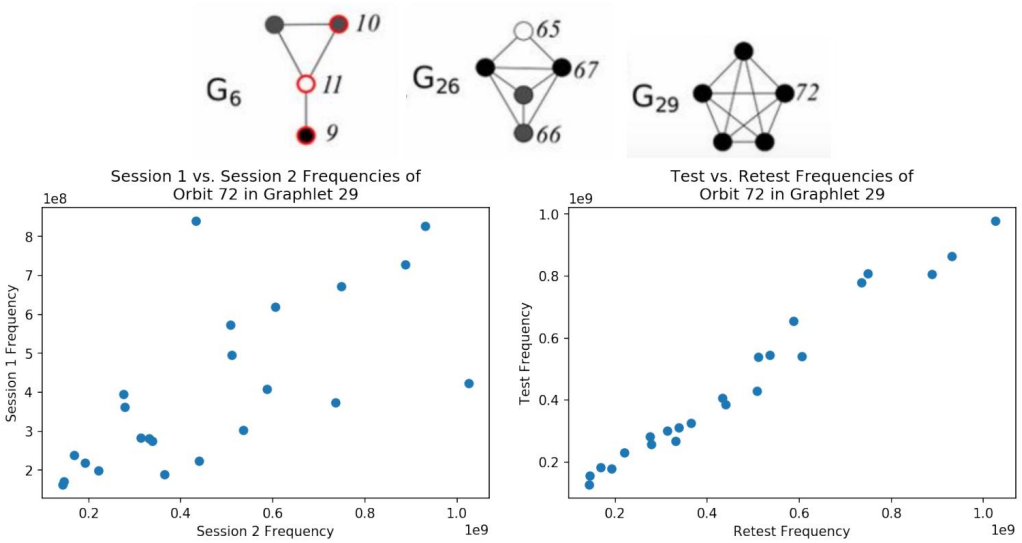

Figure 3: Frequencies of orbit 72 in Graphlet 29 (top right) across intra-test sessions (bottom left) and inter-test sessions (bottom-right). Note that the frequency of orbit 72 appearing across the network is highly correlated between test and retest scans, but less so across sessions. The other most highly correlated orbits across scans are 9, 10, 11, 65, 66, and 67, displayed at top.

While these results from our predictive analysis do suggest that topological characteristics of the functional connectome are more stable and characteristic than previously thought, our follow-up analysis analyzing differences in graphlet frequencies between depressed patients and healthy controls suggest that whatever properties are revealed by graphlet degree distributions may not necessarily relate to depressive disorders. For each of the 73 distinct orbits across the 29 possible 5-node graphlets, we ran a t-test to examine whether there was a significant difference in the average frequency of that orbit between depressed patients and healthy controls. While 11 of these orbits demonstrated significant differences at level $\alpha = 0.05$, these findings did not survive FWER control. Indeed, those orbits that appeared to be most distinct between the two groups (e.g. orbits 62, 63, and 64 with $p \approx 0.0069$) were in fact some of the least

correlated between test and retest scans within individuals. Vice versa, those motifs that were most stable/highly correlated across sessions and test/retest scans (orbits 9, 10, 11, 65, 66, 67, and 72 with Spearman correlation $p_{corr} < 1e-17$, see Figure 3) tended to display very little difference between depressed patients and controls. More work is required to better understand what behavioral, anatomical, or physiological features do in fact correlate most with these uniquely identifying graphlet degree distributions.

One final intriguing finding was that our predictive model consistently performed better when predicting retest data from test data collected weeks apart compared to predicting session 2 data from session 1 data within the same day (see Figure 3. This seemed to go against our initial intuition - we hypothesized that changes, even small ones, would occur over the course of weeks making predicting the identity of scans far in the future much more difficult than predicting the identity of scans from the same day. There may be a reasonable explanation for this, however. In the HCP protocol, the first session had R-L phase encoding rfMRI first followed by L-R phase encoding rfMRI while the second session had L-R phase encoding rfMRI followed by R-L phase encoding rfMRI. The justifications for this balancing are justified and explained in [15]. The authors seemed to believe that this balancing would have an insignificant impact on the quality and nature of the data, but our analysis seems to suggest otherwise. This is an important finding for both the HCP and other test-retest neuroimaging study designs in the future.

7 Further Work

Overall, our work and findings present a promising avenue for understanding the architecture of the functional connectome. While we hypothesized that graphlet degree distributions would relate in some way to mental health disorders like depression, our results cannot confirm such a hypothesis. Nevertheless, the remarkable accuracy with which graphlet degree distributions could uniquely identify individuals from scan to scan, even when weeks apart, is an exciting and novel contribution to the field of topological analysis of the functional connectome.

Some future work related to the robustness analysis would be to implement a probabilistic edge-removal algorithm, that follows a "higher-weighted edges are less likely to be removed than lower-weighted edges" heuristic. Additionally, further research could be done related to assess other graph properties such as average shortest path length, clustering coefficient, etc and their relationship to depression. We viewed our project as exploratory, and thought that the network topology features of robustness and graphlet degree distributions distributions made the most sense for this dataset and research question.

8 Contributions

Data collection and preprocessing were performed by Zach. The robustness analysis and the construction of connectivity networks were performed by Cooper. The graphlet degree vector analysis was performed by Scotty.

References

[1] Danielle S Bassett and Olaf Sporns. "Network neuroscience". In: *Nature neuroscience* 20.3 (2017), p. 353.

[2] Ed Bullmore and Olaf Sporns. "Complex brain networks: graph theoretical analysis of structural and functional systems". In: *Nature Reviews Neuroscience* 10.3 (2009), p. 186.

	Sess 1 vs. Sess 2			Sess 1 vs. Sess 2 with NE			Test vs. Retest		
Distance Metric	$k = 1$	$k = 3$	$k = 10$	$k = 1$	$k = 3$	$k = 10$	$k = 1$	$k = 3$	$k = 10$
RGF	0.24	0.41	0.86	0.24	0.41	0.86	0.91	1.00	1.00
GCD-11	0.13	0.31	0.76	0.13	0.31	0.76	0.91	1.00	1.00
GCD-15	0.17	0.31	0.72	0.17	0.31	0.72	0.91	1.00	1.00
GCD-58	0.17	0.41	0.90	0.17	0.41	0.90	1.00	1.00	1.00
GCD-73	0.17	0.34	0.93	0.17	0.34	0.93	1.00	1.00	1.00
GDD-A	0.07	0.14	0.31	0.07	0.14	0.31	0.09	0.26	0.65
GDD-G	0.07	0.14	0.28	0.07	0.14	0.28	0.13	0.22	0.48
Deg. Dist.	0.07	0.10	0.31	0.07	0.10	0.31	0.09	0.22	0.48
Avg. Deg.	0.03	0.17	0.66	0.03	0.17	0.66	0.30	0.48	0.96
Clust. Coef.	0.14	0.24	0.66	0.14	0.24	0.66	0.22	0.48	0.96
Diameter	0.07	0.10	0.41	0.03	0.07	0.34	0.13	0.30	0.78
Spectral	0.21	0.38	0.72	0.21	0.38	0.72	0.96	1.00	1.00

Table 1: Predictive performance under three different tasks ((i) predicting the identity of a session-2 scan from a session-1 scan in the same day, (ii) the same task but using Network Enhancement (NE) to assess whether this technique improved accuracy, and (iii) predicting the identity of a retest scan using the original test scan) using various distance metrics, including the Graphlet Correlation Distance (GCD), the Relative Graphlet Frequency Distance (RGF), the arithmetic and geometric Graphlet Degree Distribution Agreement Distances (GDD-A and GDD-G) [20]; a spectral distance metric using the eigenvalues of the network's Laplacian graph matrix [3]; and several other distance metrics based on network properties like degree distribution, clustering coefficients, and network diameter. Note that GCD-11 in this case represents a Graphlet Correlation distance with non-redundant 2-to-4 node graphlet orbits, GCD-73 represents a Graphlet Correlation distance with all 2-to-5 node graphlet orbits, and GDD-15/GDD-58 represent variations in between.

[3] Hilda Deborah, Noël Richard, and Jon Yngve Hardeberg. "A comprehensive evaluation of spectral distance functions and metrics for hyperspectral image processing". In: *IEEE Journal of Selected Topics in Applied Earth Observations and Remote Sensing* 8.6 (2015), pp. 3224–3234.

[4] David A Drachman. "Do we have brain to spare?" In: *Neurology* 64.12 (2005), pp. 2004–2005.

[5] Emily S Finn et al. "Functional connectome fingerprinting: identifying individuals using patterns of brain connectivity". In: *Nature neuroscience* 18.11 (2015), p. 1664.

[6] Guadalupe C Garcia et al. "Role of long cycles in excitable dynamics on graphs". In: *Physical Review E* 90.5 (2014), p. 052805.

[7] Matthew F Glasser et al. "A multi-modal parcellation of human cerebral cortex". In: *Nature* 536.7615 (2016), pp. 171–178.

[8] Leonardo L Gollo and Michael Breakspear. "The frustrated brain: from dynamics on motifs to communities and networks". In: *Phil. Trans. R. Soc. B* 369.1653 (2014), p. 20130532.

[9] Leonardo L Gollo et al. "Mechanisms of zero-lag synchronization in cortical motifs". In: *PLoS computational biology* 10.4 (2014), e1003548.

[10] Martijn P van den Heuvel and Olaf Sporns. "Network hubs in the human brain". In: *Trends in cognitive sciences* 17.12 (2013), pp. 683–696.

[11] *Mapping Connectomes for Disordered Mental States*. URL: https://www.humanconnectome.org/study/crhd-mapping-connectomes-disordered-mental-states.

[12] Sarah E Morgan et al. "Low-dimensional morphospace of topological motifs in human fMRI brain networks". In: *Network Neuroscience* 2.02 (2018), pp. 285–302.

[13] Jukka-Pekka Onnela et al. "Intensity and coherence of motifs in weighted complex networks". In: *Physical Review E* 71.6 (2005), p. 065103.

[14] Zhiqiang Sha et al. "Meta-Connectomic Analysis Reveals Commonly Disrupted Functional Architectures in Network Modules and Connectors across Brain Disorders". In: *Cerebral Cortex* (2017), pp. 1–16.

[15] Stephen M Smith et al. "Resting-state fMRI in the human connectome project". In: *Neuroimage* 80 (2013), pp. 144–168.

[16] Olaf Sporns and Rolf Kötter. "Motifs in brain networks". In: *PLoS biology* 2.11 (2004), e369.

[17] Michael SC Thomas and James L McClelland. "Connectionist models of cognition". In: *The Cambridge handbook of computational psychology* (2008), pp. 23–58.

[18] Martijn P Van Den Heuvel and Olaf Sporns. "Rich-club organization of the human connectome". In: *Journal of Neuroscience* 31.44 (2011), pp. 15775–15786.

[19] Bo Wang et al. "Network Enhancement: a general method to denoise weighted biological networks". In: *arXiv preprint arXiv:1805.03327* (2018).

[20] Ömer Nebil Yaveroğlu et al. "Revealing the hidden language of complex networks". In: *Scientific reports* 4 (2014), p. 4547.